Journal of New Materials for Electrochemical Systems 14, 031-037 (2011)
© J. New Mat. Electrochem. Systems

Structual Characterization of High-performance Co-polymer Lithium Storage Material by EXAFS and DFT Calculations

Qingyu Kong[1,*] Bingkun Guo[2], Francois Baudelet[1], Ying Zhu[3], Ya Mao[2], Zhaoxiang Wang[2,†], Meixiang Wan[4]
and Liquan Chen[2]

[1]Société civile Synchrotron SOLEIL,L'Orme des Merisiers, Saint-Aubin-BP 48, 91192 GIF-sur-YVETTE CEDEX France
[2]Laboratory for Solid State Ionics, Institute of Physics, Chinese Academy of Sciences, P. O. Box 603, Beijing 100190, China
[3]School of Chemistry and Environment, Beijing University of Aeronautics and Astronautics, Beijing 100191, China
[4]Organic Solid Laboratory, Institute of Chemistry, Chinese Academy of Sciences Beijing 100190, China

Received: October 10, 2010, Accepted: January 27, 2011, Available online: February 15, 2011

Abstract: *A polymer-coated Co_3O_4 composite was electrochemically induced to be a high-performance lithium-storage material. The structure of the composite before and after electrochemical charge/discharge cycling was determined by extended X-ray absorption fine structure spectroscopy (EXAFS) and density functional theory (DFT) calculations. It is found that polymer coating does not disturb the structure of commercial Co_3O_4; no coordinates are recognized between Co and the polymer in the as-prepared composite. In contrast, strong coordination occurs between Co and N atoms in the discharged composite. Data fitting to the experimental EXAFS signal yields an average atomic distance of R_{Co-N} = 1.91 Å and a Co-N coordination number of 2 for the first shell. The near edge absorption (XANES) signal also indicates the change of oxidation state of cobalt after discharge. A two-layer geometry of the Co-polymer coordinate is optimized from DFT calculations. The simulated EXAFS signal from this structure can fit the experimental data very well. It is suggested that the strong Co-N coordination weakens the C-H bonds of the polymer during discharge and makes them electrochemically active to store lithium ions, transferring the polymer to a high performance lithium-storage material.*

Keywords:

1. INTRODUCTION

Scientists worldwide are searching for new sources of clean energy to replace fossil fuels to ease the crises resulting from rapid depletion of fossil fuels and crucial environmental deterioration due to massive CO_2 emission. As one of the most important clean power sources, the application of lithium ion batteries (LIBs) has been expanded to most of today's portable electronics. A step forward is to develop LIB materials with higher specific capacity, longer cycling life and better safety characteristics for electric and hybrid electric vehicles.

Current LIB technologies are all based on inorganic electrode materials. Intensive studies have been carried out to search and develop alternative organic materials to diversify the LIB market [1-3]. However the limited thermal stability and low capacity hinder the application of the organic electrode materials. The improvement of the performances of the battery materials depends on precise understanding of their working mechanisms. We recently found that a high performance organic lithium storage material can be obtained by discharging a polymer-coated Co_3O_4 composite to 0.0V *vs*. Li^+/Li, though the cycling performances of Co_3O_4 are not satisfactory [4] and the polymer alone is electrochemically inactive [5] (the structure of the polymer will be published on the Conference). In order to understand the mechanism of the high capacity (> 1100 mAh g^{-1}), high cycling stability (the capacity is stable for over 100 cylces) and excellent rate performance of this composite, it is important to obtain accurate information on the local structure of the electrode material.

Synchrotron based X-ray absorption spectroscopy (XAS) has been employed to examine the electronic and local structures of interesting atoms in various electrode materials for LIBs [6-10]. An XAS consists of the XANES (X-ray absorption near-edge

---

To whom correspondence should be addressed:
Email: *quingyu.kong@synchrotron-soleil.fr , †zxwang@aphy.iphy.ac.cn

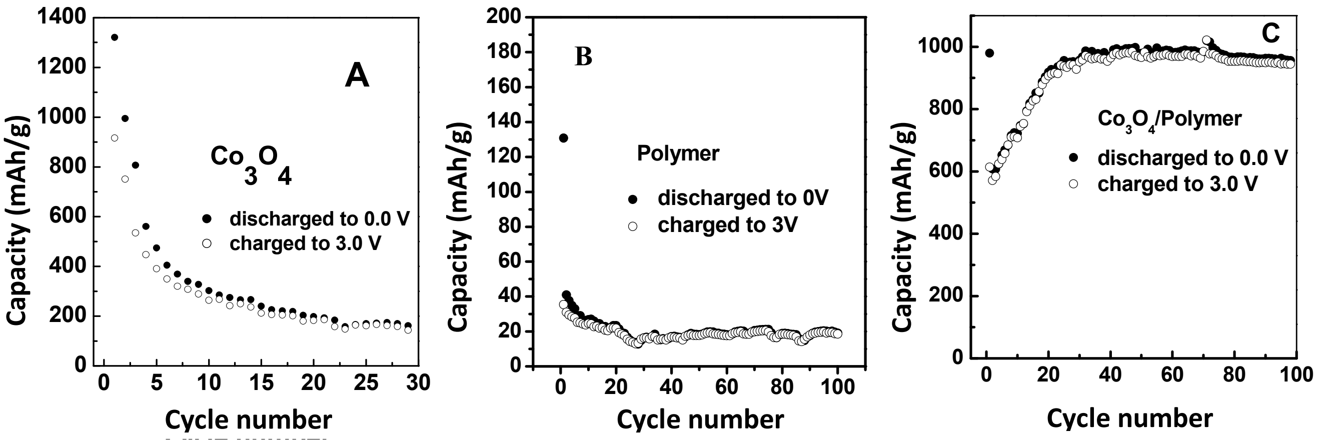

Figure 1. Comparison of the cycling performances of (A) commercial nano-Co_3O_4, (B) pure polymer, and (C) Co_3O_4/polymer composite between 0.0 and 3.0 *vs*. Li^+/Li at a current density of 0.1 mA cm^{-2}. The mass of the composite on the working electrode in this cell is 2.5 mg (the resolution of the electronic balance is 0.1 mg); the area of the square working electrode is 0.64 cm^2. The specific capacity of the commercial Co_3O_4, though very high in the first cycle, decays quickly upon further cycling. The lithium storage capacity of the pure polymer is negligible below 3.0 V *vs*. Li^+/Li. The capacity of the Co_3O_4/polymer composite is excellent indicating that polymer coating significantly improves the cycling performance of Co_3O_4.

structure) and EXAFS (extended X-ray absorption fine structure) regions. The XANES signal, which contains rich information about both the electronic and geometric structures, is very sensitive to the oxidation state and allows a good understanding of the charge transfer process. EXAFS delivers precise information about the inter-nuclear distance of the nearest neighbors from the absorbing central atom. One can obtain, in a single X-ray absorption spectrum, simultaneous information about the valence electronic structure and the nuclear arrangement of the atoms in the lithium storage materials. In this paper, we show the structural characterization of this organic electrode material before and after charge/discharge cycling using XAS and DFT calculations.

2. EXPERIMENTAL

Details about the preparation of the Co_3O_4/polymer composite and the electrochemical treatment to the material will be published in another report. The powder sample of the as-prepared and electrochemically discharged composite was grinded in an agate mortar and homogeneously spread on a piece of plexiglass in an Ar-filled glove box. The sample was sealed with Kapton foil under vacuum before taken out for EXAFS measurement.

The structures of the Co_3O_4/polymer composite before and after discharge were analyzed with EXAFS spectroscopy. The X-ray absorption spectra were recorded in the transmission mode at the Co *k*-edge. The spectra of a metallic cobalt foil recorded at ambient pressure and temperature were used for energy calibration. The quality of the spectra at the Co *k*-edge allows EXAFS analysis up to 300 eV beyond the edge. All measurements were performed at the optical dispersive EXAFS (ODE) beamline at the Soleil synchrotron, France. Briefly, X-ray radiation is produced by a bending magnetic field, then focused vertically by a curved mirror (single silicon crystal coated with Cr plus Rh) from the optical hutch to the sample. A dispersive monochromator (Si(111) crystal, Bragg configuration) is used to focus the X-ray horizontally. Its plane is perpendicular to that of the mirror. In such a configuration, the focused X-ray covers a brand energy range (1100 eV at Co *k*-edge), an EXAFS spectrum with full energy range can be obtained from a single exposure to the CCD detector. At Co *k*-edge (7.7089 keV), a round spot of 30 µm (FWHM) on the sample can be obtained by the focus mirror and the monochromator, with a flux of 3×10^9 photons/s/eV.

The EXAFS signals were collected with a CCD array detector (SPEC-10, Princeton Instruments) in the transmission mode. The exposure time for a single frame is 100 ms. Each spectrum was averaged over 300 frames to get a reasonable single to noise ratio.

Density functional theory (DFT) and *ab initio* calculations were conducted with the Gaussian 09 program [11], the Becke three-parameter hybrid functional with the Lee-Yang-Parr correlation corrections (B3LYP) [12,13], the Becke three-parameter hybrid functional with the Perdew and Wang's 1991 gradient-corrected correlations (B3PW91) [12,14], and the Hartree-Fock (HF) [15] methods with the all electron basis set 6-311++G(d,p) for single layer and 6-31G(d) for double layers structures, were used for the calculations.

3. RESULTS AND DISCUSSION

Galvanostatic cycling tests reveal that the specific capacity of the commercial Co_3O_4, though very high in the first cycle, decays quickly upon further cycling (Fig. 1A). The lithium storage capacity of the pure polymer is negligible below 3.0 V *vs*. Li^+/Li (Fig. 1B). Polymer coating significantly improves the cycling performance of commercial Co_3O_4 (Fig. 1C). In addition, the specific capacity increases continuously from *ca*.650 to *ca*.1000 mAh/g in the first 30 cycles. Scanning electron microscopic(SEM) images show that the commercial Co_3O_4 aggregate severely after charge/discharge cycling (Fig. 2A and B). In contrast, the buffering of the elastic polymer coating to the large volume variation of the Co_3O_4 particles and the tight binding of the conductive polymer to

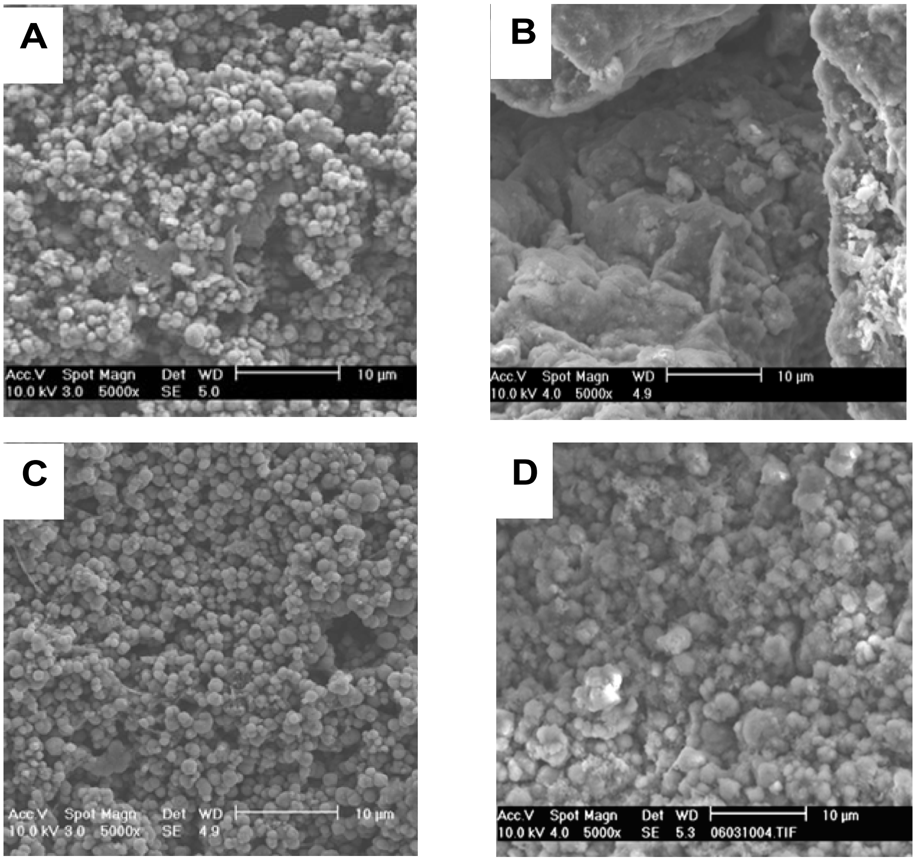

Figure 2. The scanning electron microscope(SEM) images of commercial Co_3O_4 on the as-prepared electrode sheet (A) and on an electrode sheet after 30 galvanostatic cycles (B), the Co_3O_4/polymer composite on an as-prepared electrode sheet (C) and on an electrode sheet after 35 cycles (D).

the nanoparticles prevent the aggregation of the Co_3O_4 nanoparticles effectively (Fig. 2C and D). The high stability of the polymer coated Co_3O_4 nanoparticles explains its excellent performance during charge/discharge cycling on one hand, detailed mechanism requires accurate electronic and structural information of the Co_3O_4/polymer compound.

Direct electronic and local structures of the Co_3O_4/polymer composite before and after cycling were determined with XAS at the Co *k*-edge. Fig. 3 shows the normalized absorption spectrum $\chi_\mu(E)$, absorption coefficient $k\chi(k)$, and the magnitude of Fourier-transformed $|\chi(R)|$ of the Co_3O_4/polymer composite before and after charge/discharge cycling. The red curves in the top and middle panels of Fig. 3 are the experimental EXAFS spectra of pure Co_3O_4 and metallic Co, respectively. Fig. 3 (bottom) compares the normalized spectra $\chi_\mu(E)$ of the composite before and after cycling. The obvious difference demonstrates the structural change of the material due to the electrochemical reaction. The pre-edge shift (inset) indicates that the oxidation state of Co decreases after electrochemical discharge, consistent with previous report that Co_3O_4 is reduced during lithium insertion [16]. The intersection between the two curves (inset) also indicates that the oxidation state of Co in the discharged Co_3O_4/polymer composite is a mixture (of probably Co(II) and Co(III)). Direct experimental data analysis shows that the EXAFS signal of the as-prepared Co_3O_4/polymer composite is very similar to that of Co_3O_4 (red curve in Fig. 3 top). Theoretical EXAFS signals calculated from the crystal structure of Co_2O_3 and DFT-calculated Co-polymer coordinates cannot produce reasonable fitting to the EXAFS signals of the as prepared Co_3O_4/polymer composite. These indicate that polymer coating does not change the structure of Co_3O_4.

Previous Co *k*-edge EXAFS studies showed that Co_3O_4 is first reduced to Co(II) and finally to metallic cobalt upon lithium insertion [16]. Therefore, metallic cobalt is firstly considered to be the product of the electrochemical reduction of the Co_3O_4/polymer composite. Fig. 3 (middle) compares the experimental EXAFS signals of the discharged Co_3O_4/polymer composite with that of metallic Co foil. Although some features similar to that of metallic Co are present, metallic Co alone cannot produce satisfactory fitting. Clearly, the first peak at 1.91 Å in the Fourier-transformed $|\chi(R)|$ (Fig. 3 middle), representive of the first-shell neighbors of the excited Co atoms, cannot be reproduced from pure metallic Co since the nearest Co-Co distance is 2.5 Å in crystalline metallic Co (red curve of the Fourier-transformed $|\chi(R)|$ in Fig. 3 middle). Theoretical EXAFS signal calculated from CoO can not fit the experimental data of the discharged Co_3O_4/polymer composite either.

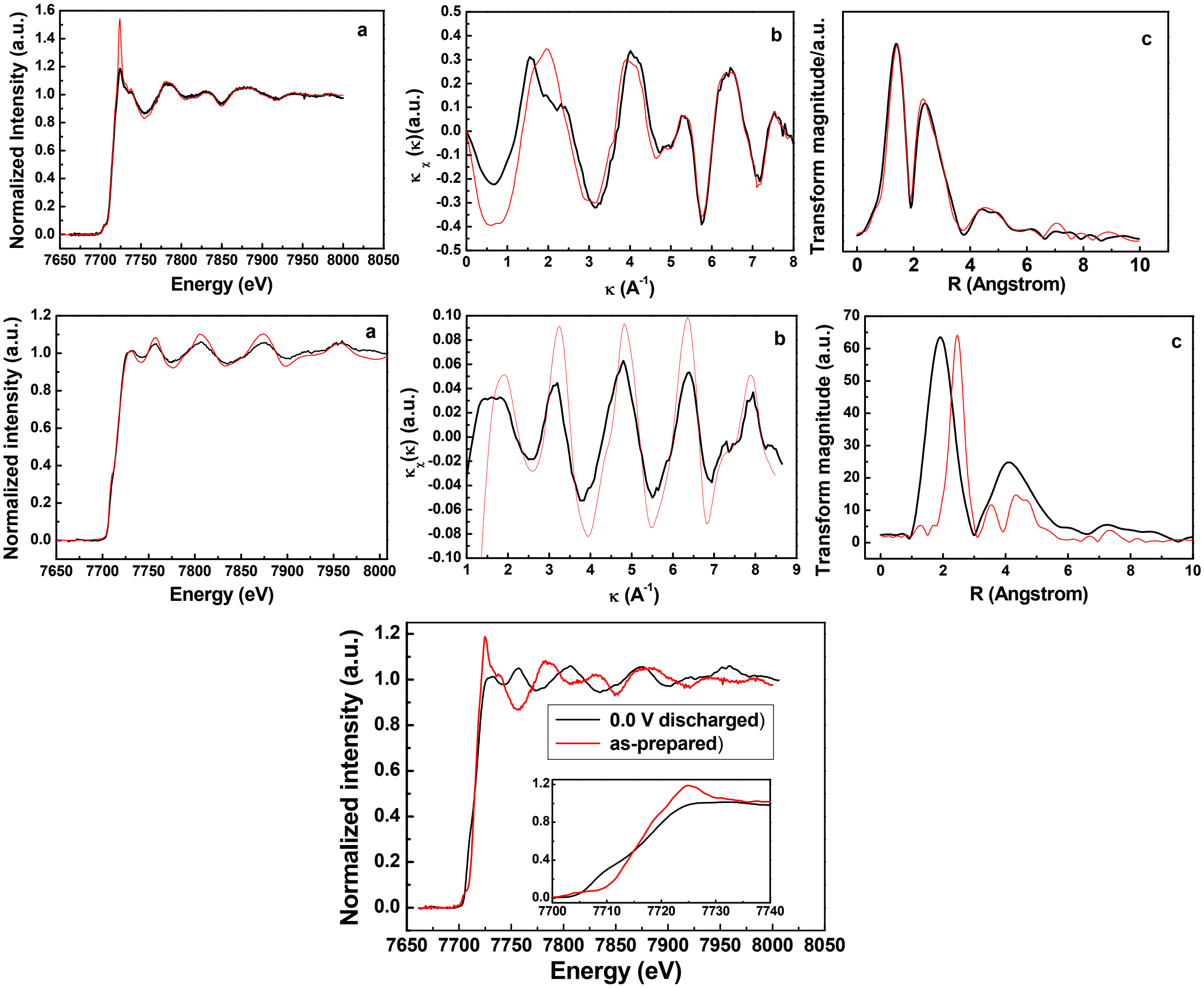

Figure 3. The EXAFS spectra of fresh Co_3O_4/polymer composite (top), the Co_3O_4/polymer composite discharged to 0.0 V *vs.* Li^+/Li (middle) and the comparison of the normalized spectra of the as-prepared and 0.0 V-discharged Co_3O_4/polymer composite (bottom). (a) normalized spectrum as a function of energy, (b) the absorption coefficient *kc(k)*, and (c) the Fourier transformed magnitude |*c(R)*|. The pre-edge shift (inset) indicates that the oxidation state of Co decreases after discharge. The red curves in the top and middle panels are experimental EXAFS spectra of pure Co_3O_4 and metallic Co respectively.

Yuasa [17] and Bashyam [18] chemically synthesized cobalt-polymer (Co-polymer) coordinates and used them as electrocatalyst for fuel cells. Although the lithium storage capacity of their coordinate-containing material was found negligible, their reports remind us that similar coordinates might also be formed in the electrochemically cycled Co_3O_4/polymer composite. Model structures, in which each Co atom is coordinated with 2 [18] or 4 [17] N atoms, were calculated with the B3LYP/6-311++G(d,p) method. The optimized structures are shown in Fig.4a and b respectively. To determine the coordination numbers of the Co atom in the discharged sample, EXAFS signals were simulated with FEFF 8.0 program from the DFT optimized structures in Fig. 4a and b. The simulated results were compared with the experimental EXAFS signal. Since the N atoms are within the first-shell neighbors of the excited Co atom, only the first peak in the Fourier-transformed magnitude $|\chi(R)|$ is selected to evaluate the fitting quality (Fig. 5). Apparently the Bashyam model produces a quite good fit to the first-shell EXAFS signal of the experimental data (Fig. 5a), while the Yuasa model cannot give a reasonable fit (Fig. 5b). From the data fitting to the experimental EXAFS signals using DFT optimized structures (Fig. 4), the coordination numbers of the Co atom is determined to be 2. However, theoretical EXAFS signal calculated from this one-layer Co-Polymer coordinate cannot reproduce the second-shell peak around 4 Å (Fig. 5a). A bulk structure was then calculated with the B3LYP/6-31G(d) method, its top and side views are shown in Fig. 6. In this configuration, each Co atom is coordinated with 2 N atoms in the layer-structured coordinate (Fig. 6a), the two neighboring slabs are connected with O atoms via the Co atom in the coordinate (Fig. 6b). Theoretical EXAFS signal calculated from this geometry produces a reasonable fitting to the experimental data

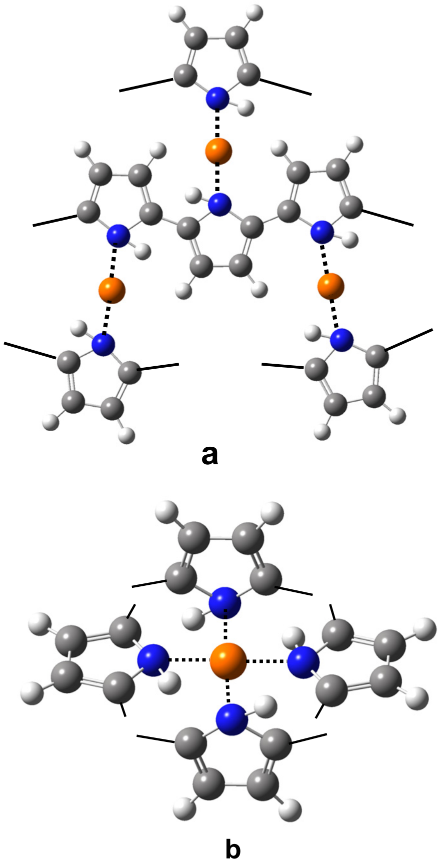

Figure 4. DFT optimized structures: (a) the Bashyam model: each Co atom is coordinated with 2 N atoms; (b) the Yuasa model, each Co atom is coordinated with 4 N atoms. Color note: orange for Co, blue for N, grey for C, and white for H in both schematics. The B3LYP/6-311++G(d,p) method was used for the DFT calculations.

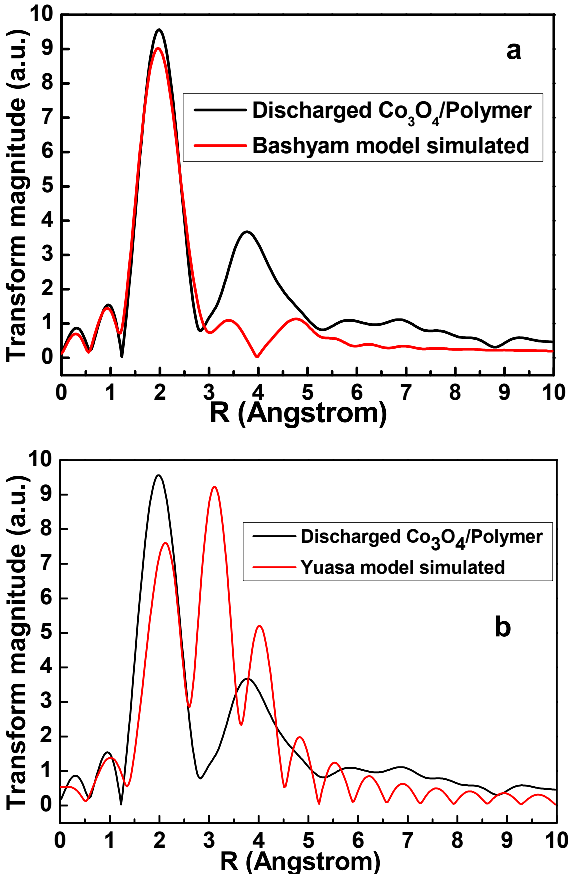

Figure 5. Comparison of the experimental EXAFS signal of the discharged Co_3O_4/polymer composite (black curves) with the simulated results (red curves) based on (a) the Bashyam model where each Co atom is coordinated with 2 N atoms (Fig. 4a) and (b) the Yuasa model where each Co atom is coordinated with 4 N atoms (Fig. 4b). Only the first peak is used to evaluate the fitting quality.

as shown in Fig. 7a. To consider the formation of metallic Co in the discharged Co_3O_4/polymer composite as mentioned above, a least-squares refinement was applied to evaluate the concentration ratio of the free metallic Co and Co-polymer ligand by fitting the experimental EXAFS signal with these two components. The refinement shows that 56.8% of the total signals come from Co-polymer ligand and 43.2% from free metallic Co. The fitting results are shown in Fig. 7b. The least squares refinement is defined as:

$$\chi^2 = \sum_{Q} \frac{(S_{sim}(R) - S_{data}(R))^2}{2\sigma_R^2} / (N - p - 1)$$

Where $S_{sim}(R)$ is the simulated signal, $S_{data}(R)$ the experimental data, σ the standard deviation, N the number of R-points and p the number of free parameters. The figure of merit χ^2 is used to evaluate the fitting quality. In the least-square refinement, the experimental EXAFS signal of charged/discharged Co_3O_4/polymer composite was fitted by including both the experimental EXAFS signal of metallic Co and the theoretical EXAFS signal calculated from the Co-polymer coordinate as shown in Fig. 6. The concentration ratios of these two components were evaluated until a best fitting (smallest χ^2) was obtained. The least-squares refinement was successfully applied in time-resolved X-ray scattering measurement to determine the concentration ratios of transient molecules [19,20].

Data fitting of the EXAFS signal of the charged/discharged Co_3O_4/poymer composite indicates that a chemical bond is formed between Co and the N atoms of the polymer, with a Co-N bond length of 1.91 Å. The first-shell coordination number of the Co atom is 2. A DFT optimized structure (Fig. 6) produces a reasonable fit to the experimental EXAFS signal (Fig. 7a), suggesting that such structures could be formed during the electrochemical reaction of the Co_3O_4/polymer composite.

Our TG analysis has shown that the content of the polymer in the as-prepared Co_3O_4-polymer composite is 70wt.%. Therefore, the contribution of the polymer to the specific capacity of the composite should be over 1100 mAh g^{-1} (350 ¸ 0.3 = 1,166 mAh g^{-1}). This means that each polymer unit (the polymer unit will be published in the Conference) can store more than 2.7 Li ions. Considering that

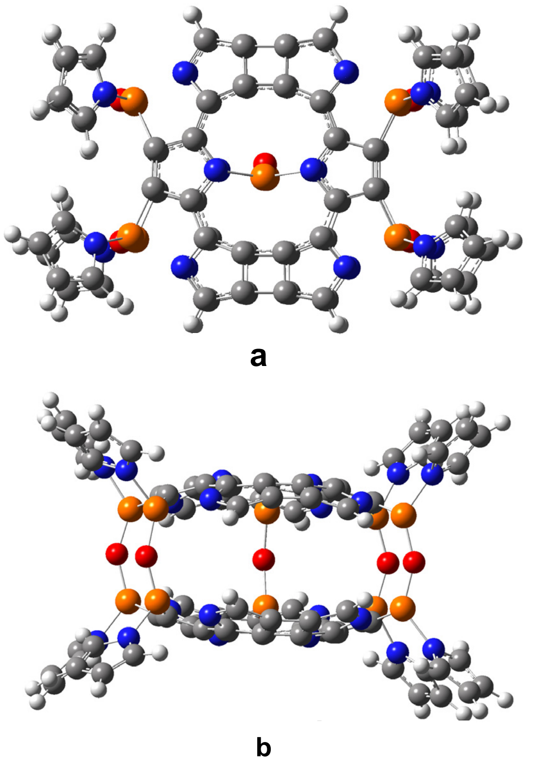

Figure 6. The top view (a) and the side view (b) of the DFT-calculated configuration of the Co-polymer coordinates using the B3LYP/6-31G(d) method. Colors of the ball: red for O, orange for Co, blue for N, grey for C, white for H.

all the polymer molecules cannot react with Li (the polymer molecules far from the Co_3O_4 particle might not be able to form a coordinate with the Co atom), each unit should store 3 lithium ions or more. However, no information about the position of the lithium atoms in the Co-polymer coordinate can be obtained from our EXAFS measurement due to its low Z number. A DFT calculated Li-doped Co-polymer coordinate is shown in Fig. 8 to illustrate the possible positions of the lithium atoms in the coordinate. In this configuration, 2 lithium atoms are connected to the C atoms at the meta-positions of the N atom and the 3rd lithium atom is located above or below the ring of the polymer unit.

4. CONCLUSION

In summary, Co-polymer coordinated ligand have been electrochemically formed and are proved a high-performance lithium storage material. To our knowledge, no metal-polymer coordinate has been reported as a lithium storage material and no organic electrode materials can have such high specific capacity and cycling stability. Our findings might open a new avenue for the search of high-performance lithium-storage materials and possibly paves ways for preparing electrocatalysts with higher efficiencies than what Bashyam suggested.

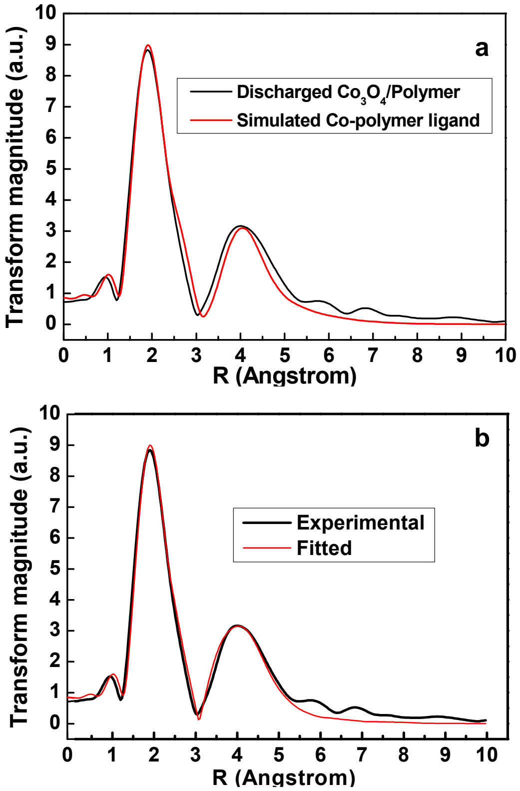

Figure 7. Comparison of the experimental EXAFS signal (thick&black) of Co_3O_4/polymer composite discharged to 0.0 V vs. Li^+/Li with the simulated signals (thin&red) of (a) the Co-polymer coordinates, and (b) combination of metallic Co and the Co-polymer coordinates with least-squares refinement method. The simulation was carried out with the FEFF8 code.

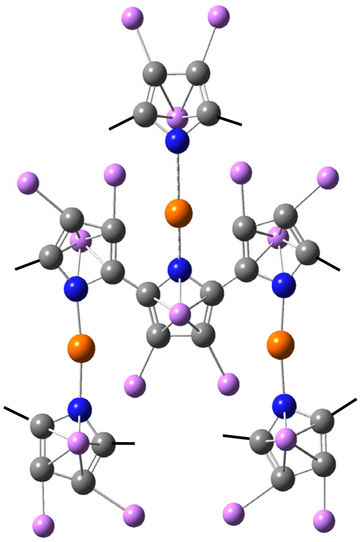

Figure 8. DFT optimized Li-doped Co-polymer coordinate, each unit is doped with 3 Li atoms, 2 of which are located at the mesa-position of the N and the third is above or below the polymer ring. This structure is calculated by the B3LYP/6-311+G(d) method. Note: orange for Co, blue for N, grey for C, pink for Li.

6. ACKNOWLEDGEMENTS

The authors would like to thanks Dr. Philippe Martinez for his help with Gaussian calculations, Valerie BRIOIS and Amelie ROCHET for measuring the EXAFS spectra of metallic Co and pure Co_3O_4. This work was financially supported by the National 973 Program (No.2002CB211800 and 2009CB220100) and the National Science Foundation of China (NSFC No.50472072 and 20974120).

REFERENCES

[1] A.G. MacDiarmid, L.S. Yang, W.S. Huang, B.D. Humphrey, Synth. Metals, 18, 393 (1987).

[2] P. Novak, K. Muller, K.S.V. Santhanam, O. Haas, Chem. Rev., 97, 207 (1997).

[3] M. Armand, S. Grugeon, H. Vezin, S. Laruelle, P. Ribiere, P. Poizot, J.M. Tarascon, Nature Mater., 8, 120 (2009).

[4] P. Poizot, S. Laruelle, S. Grugeon, L. Dupont, J.M. Tarascon, Nature 407, 496 (2000).

[5] M.D. Levi, Y. Gofe, A.D. Aurbach Polym. Adv. Technol., 13, 697 (2002).

[6] C. Delmas, J.P. Peres, A. Rougier, A. Demourgues, F. Weill, A. Chadwick, M. Broussely, F. Perton, P. Biensan, P. Willmann, J. Power Sources, 68, 120 (1997).

[7] I. Nakai, T. Nakagome, Electrochem. Solid-State Lett., 1, 259 (1998).

[8] W.S. Yoon, K.B. Kim, M.G. Kim, M.K. Lee, H.J. Shin, J.M. Lee, J.S. Lee, C.H. Yo, J. Phys. Chem. B, 106, 2526 (2002).

[9] W.S. Yoon, M. Balasubramanian, K.Y. Chung, X.Q. Yang, J. McBreen, C.P. Grey, D.A. Fischer, J. Am. Chem. Soc., 127, 17479 (2005).

[10]W.S. Yoon, K.Y. Chung, J. McBreen, K. Zaghib, X.Q. Yang, Electrochem. Solid-State Lett., 9, A415 (2006).

[11]Gaussian 09, Revision A.1, M.J. Frisch, G.W. Trucks, H.B. Schlegel, G.E. Scuseria, M.A. Robb, J.R. Cheeseman, G. Scalmani, V. Barone, B. Mennucci, G.A. Petersson, H. Nakatsuji, M. Caricato, X. Li, H.P. Hratchian, A.F. Izmaylov, J. Bloino, G. Zheng, J.L. Sonnenberg, M. Hada, M. Ehara, K. Toyota, R. Fukuda, J. Hasegawa, M. Ishida, T. Nakajima, Y. Honda, O. Kitao, H. Nakai, T. Vreven, J.A. Montgomery, Jr., J. E. Peralta, F. Ogliaro, M. Bearpark, J.J. Heyd, E. Brothers, K. N. Kudin, V.N. Staroverov, R. Kobayashi, J. Normand, K. Raghavachari, A. Rendell, J.C. Burant, S.S. Iyengar, J. Tomasi, M. Cossi, N. Rega, J.M. Millam, M. Klene, J.E. Knox, J.B. Cross, V. Bakken, C. Adamo, J. Jaramillo, R. Gomperts, R.E. Stratmann, O. Yazyev, A.J. Austin, R. Cammi, C. Pomelli, J. W. Ochterski, R.L. Martin, K. Morokuma, V.G. Zakrzewski, G. A. Voth, P. Salvador, J.J. Dannenberg, S. Dapprich, A.D. Daniels, O. Farkas, J.B. Foresman, J.V. Ortiz, J. Cioslowski, and D.J. Fox, Gaussian, Inc., Wallingford CT, 2009.

[12]A.D. Becke, J. Chem. Phys., 98, 5648 (1993).

[13]C. Lee, W. Yang, R.G. Parr, Phys. Rev. B, 37, 785 (1988).

[14]J.P. Perdew, K. Burke, Y. Wang, Phys. Rev. B, 54, 16533 (1996).

[15]J.A. Pople, R.K. Nesbet, J. Chem. Phys., 22, 571 (1954).

[16]A.P. Connor, J.T.S. Irvine, Electrochimica Acta, 47, 2885 (2002).

[17]M. Yuasa, A. Yamaguchi, H. Itsuki, K. Tanaka, M. Yamamoto, K. Oyaizu, Chem. Mater., 17, 4278 (2005).

[18]R. Bashyam, P. Zelenay, Nature, 63, 443 (2006).

[19]Q.Y. Kong, J.H. Lee, A. Plech, M. Wulff, H. Ihee, M.H.J. Koch, Angew. Chem. Int. Ed., 47, 5550 (2008).

[20]Q.Y. Kong, J.H. Lee, K.H. Kim, J. Kim, M. Wulff, H. Ihee, M. H.J. Koch, J. Am. Chem. Soc., 132, 2600 (2010).